

Efficiency of Emerging Photovoltaic Devices under Indoor Conditions

Markus C. Scharber

Emerging photovoltaic (PV) technologies are considered to be excellent candidates to be used as power sources for indoor and low-light applications. The already demonstrated high power conversion efficiencies (PCEs) and the potential to manufacture perovskite, organic, or dye-sensitized solar cells at low cost make them particularly interesting. In this work, the maximum PCE of PV devices under low-light conditions is explored. The role of spectral mismatch, non-radiative recombination, and parasitic Ohmic losses is investigated. The performed calculation provides guidelines to improve the low-light performance of PV devices for ambient light. In addition, a simple measurement procedure for the indoor PCE is discussed.

1. Introduction

Wearable and portable electronic devices, wireless sensors, and the many components comprising the so-called internet of things have already become important tools in our daily lives.^[1,2] It is expected that the application of smart sensor networks monitoring, e.g., environmental pollution or processes in industry or logistics will significantly increase the number of low-power electronic components in the future. Today, mostly batteries are used as power sources for these devices. This requires periodic replacement or recharging of the power sources. Considering the large number of distributed sensor networks or wearable health diagnostics devices that will be used in the future, it may not be desirable from an environmental, resource, safety, and cost perspective to power all these systems with batteries. As most of these systems will be operated predominantly indoors, there is a limited number of energy harvesting technologies available to provide power remotely. Heat (thermoelectricity),^[3–5] mechanical vibration/movement (piezo- and tribo-electricity),^[6,7] harvesting energy from radio frequencies available in the environment,^[8] and ambient light (photovoltaics [PVs])^[9] have been considered in detail. Under

typical indoor conditions, all of them provide only moderate/low power density, and converting ambient light into electricity appears to be the most promising power source.


PV is a technology that directly converts light into electricity. PV is considered to be one of the key renewable energy sources in the future and is already widely used to convert solar radiation into electricity. PV devices comprise at least a semiconductor absorber and two electrical contacts. To achieve the best performance, the bandgap of the semiconductor needs to be matched to the spectrum of the radiation the device

is exposed to under operation. There is a critical difference between indoor and outdoor PV systems as the emission spectra and power densities of the light sources available to them are different. While the solar radiation spectrum is widely distributed from the ultraviolet (UV) to the infrared (IR) region over the range of 280–4000 nm, the emission spectra of indoor lighting generated by fluorescent lamps (FLs) or white light-emitting diodes (LEDs) are typically limited to the visible range of 400–700 nm.^[10] Therefore, the bandgap of PV devices optimized for indoor radiation can be much larger compared to solar cells optimized for outdoors. In addition, the incident power density of these indoor light sources (typically 0.1–1 mW cm⁻²) is approximately two to three orders of magnitude lower compared to solar radiation (AM 1.5G, 100 mW cm⁻²) allowing different device designs for indoor and outdoor PV.

The low power density available indoors does limit also the applicability of PV cells. The only devices with low power consumption can be powered self-sufficiently. Often supercapacitors or small batteries will be added as energy buffers. As the available radiation density is low, the power conversion efficiency (PCE) of indoor solar cells should be as large as possible. This can be achieved by matching the optical properties of the solar cell to the spectrum of the indoor light source. For this various emerging PV technologies,^[11,12] significant advantages are offered. While the bandgap of silicon- or CdTe-based solar cells is fixed and almost ideal for harvesting solar radiation, the bandgap of, e.g., organic, dye-sensitized, or perovskite solar cells can be easily adjusted by tuning the chemistry of the semiconductors. In addition, the manufacturing processes of most emerging PVs are believed to be very simple, cheap, and potentially environmentally friendly. Devices can be processed on flexible and lightweight substrates simplifying their integration into sensor or portable devices.^[13] These advantages have led to a renaissance of indoor PV (IPV) driven by the research community working on emerging solar cell technologies.

M. C. Scharber

Linz Institute for Organic Solar Cells
Altenbergerstrasse 69, 4040 Linz, Austria
E-mail: markus_clark.scharber@jku.at

 The ORCID identification number(s) for the author(s) of this article can be found under <https://doi.org/10.1002/solr.202300811>.

© 2023 The Authors. Solar RRL published by Wiley-VCH GmbH. This is an open access article under the terms of the Creative Commons Attribution-NonCommercial License, which permits use, distribution and reproduction in any medium, provided the original work is properly cited and is not used for commercial purposes.

DOI: 10.1002/solr.202300811

In this manuscript, the efficiency limits of IPV's will be discussed. The importance of radiative recombination, the role of shunt and series resistance, and the effect of a bandgap mismatch will be addressed. In addition, a procedure to determine the PCE of solar cells operated under indoor conditions is proposed. As there are no standard measurement procedures, calibrated light sources, and photodetectors available for the characterization of solar cells under indoor conditions, different light sources, light intensities, and measurement tools have been used in reports available in the literature. This makes a comparison of results very difficult.

2. Efficiency Limit of IPV

In 1961, W. Shockley and H. J. Queisser reported the "Detailed Balance Limit of Efficiency of p-n Junction Solar Cells".^[14] In their calculations, they assumed perfect absorption with each photon creating exactly one electron-hole pair, perfect collection of carriers, and radiative recombination as the only allowed recombination mechanism. The solar spectrum was approximated by the radiation of a black body with a temperature of 6000 K while the solar cell was operated at room temperature. Shockley and Queisser report maximum PCEs in the range of 30%.

For the calculations presented here, a model proposed by Rau, Vandewal et al. and Tress et al.^[15–17] which includes the effect of non-radiative recombination, is applied. Wolfram Mathematica 11.2 was used for the calculations. In the following, briefly the set of equations is discussed (for a more elaborated derivation, see ref. [15]). Equation (1a–c) describes the photocurrent density J_{PH} , recombination current density in thermal equilibrium J_0 , and the voltage dependence of the current density J .

$$J_{PH} = q \int EQE_{PV}(\lambda) * \Phi_{LS}(\lambda) d\lambda \quad (1a)$$

$$J_0 = q \int EQE_{PV}(\lambda) * \Phi_{BB}(\lambda) d\lambda \quad (1b)$$

$$J(V) = \frac{J_0}{EQE_{EL}} \left(e^{\frac{qV}{k_B T}} - 1 \right) - J_{PH} \quad (1c)$$

where q is the unit charge and EQE_{PV} is the external quantum efficiency of the solar cell, which is defined as the number of electrons delivered by the solar cell under short-circuit conditions divided by the number of incident photons. In this work, EQE_{PV} is equal to 0 for every wavelength $\lambda > \lambda_G$ and constant (often equal to 1) for $\lambda < \lambda_G$. λ_G defines the onset of absorption of the photoactive material. Φ_{LS} is the spectral photon flux provided by the illumination source; Φ_{BB} is the spectral photon flux from the environment assuming an ideal black-body radiation at 300 K. V is the voltage applied to the device and EQE_{EL} is the external electroluminescence quantum yield given by the number of photons extracted from the cell divided by the number of injected electrons. EQE_{EL} can be measured in the dark when the device operates as an LED driven with the injection current comparable to the recombination current of the solar cell when operated under illumination and open-circuit conditions. EQE_{EL} should be closely related to the radiative recombination quantum

yield in the semiconductor material. For the calculations, a light source which delivers a constant spectral photon flux between 400 and 700 nm (Figure S1, Supporting Information) is assumed. This is an idealized illumination spectrum which simplifies the performed calculations and includes the contributions of high and low energy photons which only moderately contribute to the illumination.

$$L = K_m \int \frac{hc}{\lambda} \Phi_{LS}(\lambda) V(\lambda) d\lambda \quad (2)$$

To adjust the illuminance of the light source to typical indoor levels, Equation (2) is used. Here, L is the illuminance, K_m is a constant representing the maximum luminous efficiency ($K_m = 683 \text{ lm W}^{-1}$), $V(\lambda)$ denotes the spectral luminous efficiency function for human photopic vision, and h is the Planck constant. To account for resistive losses, a simple replacement circuit with a shunt and a series resistance (R_{SH} , R_s) is used. This results in the current-voltage characteristics described by Equation (3).

$$J(V) = \frac{J_0}{EQE_{EL}} \left(e^{\frac{q(V-JR_s)}{k_B T}} - 1 \right) + \frac{(V - JR_s)}{R_{SH}} - J_{PH} \quad (3)$$

Figure 1 illustrates the effect of non-radiative recombination on the solar cell performance. The calculations were performed using Equation (1a–c). The illuminance was set to 1000 Lux which corresponds to an intensity of 4.27 W m^{-2} . In addition, for all calculations, EQE_{PV} is equal to 0 for every wavelength $\lambda > \lambda_G$ and equal to 1 for $\lambda < \lambda_G$. This corresponds to a solar cell with ideal optical properties.

The calculations show that the maximum efficiency is achieved when the absorption of the solar cell and the emission spectrum of the light source perfectly overlap. The maximum is found to be quite distinct and a small mismatch leads to significantly lower efficiencies. Reducing the EQE_{EL} leads to a reduction ($\approx 60 \text{ mV}$ per decade) of the open-circuit voltage and the electrical fill factor. The short-circuit current is not affected. Overall, the maximum conversion efficiency drops from $\approx 53\%$ ($EQE_{EL} = 1$) to $\approx 38\%$ ($EQE_{EL} = 10^{-6}$). An EQE_{EL} in the range of 10^{-3} is typically found for perovskite solar cells^[18] while organic solar cells usually show much smaller values for EQE_{EL} ($\approx 10^{-6}$).^[19] The calculated recombination current density J_0 as a function of absorption onset of the semiconductors is shown in Figure S2, Supporting Information. In contrast, changes in the light intensity do not have a significant impact on the efficiency of an ideal solar cell. PCEs of $\approx 55\%$ and $\approx 52\%$ are calculated for an illuminance of 5000 Lux and 200 Lux, respectively (Figure S3, Supporting Information). Using Equation (3), the influence of the series and parallel resistors can be evaluated. **Figure 2a** summarizes the effect of R_s on the device PCE. For the calculations, R_{SH} was set to $10 \text{ G}\Omega \text{ cm}^2$, the illuminance to 1000 Lux, and EQE_{EL} to 1. Due to the very small photocurrents generated by the device, the Ohmic losses over R_s are very small and the PCE barely changes even for $R_s = 200 \Omega \text{ cm}^2$. For comparison, for state-of-the-art perovskite or organic solar cells comprising a transparent indium-doped tin oxide (ITO) and a thin metal electrode, R_s values in the range of $1 \Omega \text{ cm}^2$ are observed. The presented calculations show that, for indoor devices, the

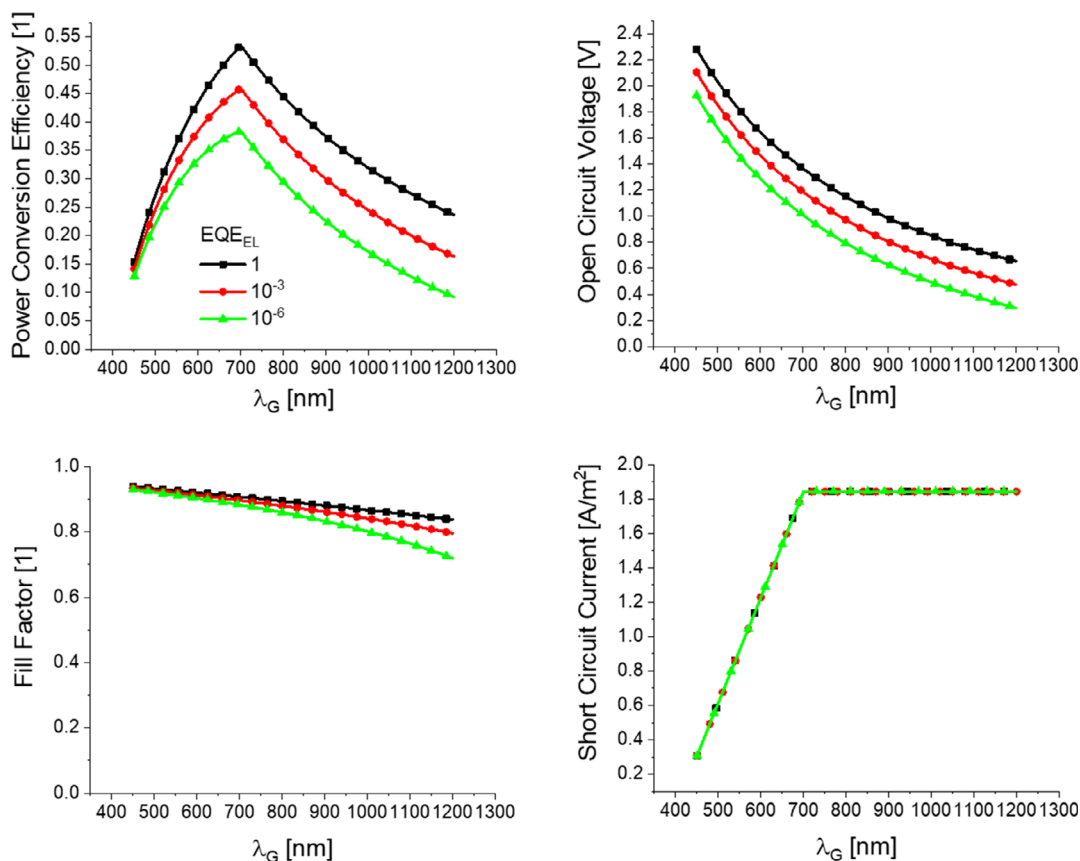


Figure 1. Calculated power conversion efficiency (PCE), open-circuit voltage, electrical fill factor, and short-circuit current density as a function of the absorption onset wavelength of the solar cell. For the calculations, Equation (1a–c) was applied. An illumination source with constant photon flux between 400 and 700 nm, an illuminance of 1000 Lux and $EQE_{PV} = 1$ was assumed.

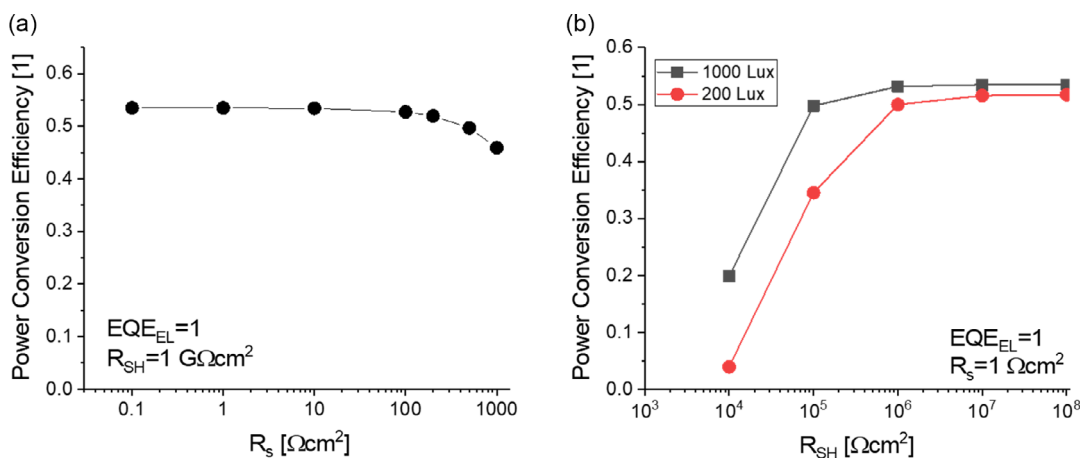


Figure 2. a) Effect of the series resistance R_s and b) effect of the shunt resistance R_{SH} on the PCE of an ideal solar cell. For the calculations, Equation (1a–c) and (3) were applied and EQE_{PV} was set to 1.

expensive ITO electrode could be replaced by a less conductive transparent layer, e.g., the conductive polymer poly(3,4-ethylenedioxythiophene) polystyrene sulfonate (PEDOT:PSS).

PEDOT:PSS can easily be deposited on different substrates by simple coating or printing processes. Thin layers are highly

transparent and form flexible and stretchable electrodes. The role of the shunt resistance R_{SH} is illustrated in Figure 2b. The PCEs calculated for 200 Lux and 1000 Lux are plotted versus R_{SH} . As a rule of thumb, R_{SH} should be much larger than V_{oc}/J_{sc} . Considering the ideal solar cell from above ($R_s \ll 1 \Omega \text{ cm}^2$,

$R_{SH} > 1 \Omega \text{ cm}^2$), we find that $V_{oc}/J_{sc} \approx 7.4 \text{ k}\Omega \text{ cm}^2$ for 1000 Lux and $\approx 36 \text{ k}\Omega \text{ cm}^2$ for 200 Lux illuminance. Figure 2b confirms these findings. To maintain the full performance, the leakage current through the resistor R_{SH} needs to be much smaller compared to the photocurrent delivered by the solar cell. This means that indoor devices operated at very low-light intensities (a few hundred lux) need to have a shunt resistance in the $M\Omega \times \text{cm}^2$ range. This can be a challenge, e.g., for organic but also perovskite solar cells. Due to the very thin photoactive layer ($< 1 \mu\text{m}$), it is a common issue that the absorber layer does not fully cover the substrate. Pinholes and defects leading to microshunts are formed around substrate imperfections, due to particles present in the printing ink substrate or formed during the device manufacturing process. For large R_{SH} , the number of shunt defects needs to be as small as possible. There are different device designs^[20] (pin or nip) available for organic photovoltaic (OPV) and perovskite solar cells which can be utilized for the optimization of the shunt resistance for a given absorber material. The quality of the photoactive layer of a solar cell can easily be evaluated using electroluminescence spectroscopy or photothermal imaging.^[21,22] In some cases, applying short voltage pulses to the solar cell can remove microshunts and improve the low-light performance of the device.^[23]

The performed calculation shows that high PCEs can be achieved by 1) matching the semiconductor absorption to the emission spectrum of the used light source; 2) selecting semiconductors with high radiative recombination yield; and 3) manufacturing devices with a large shunt resistance.

All these requirements also apply to PV devices used for solar radiation harvesting. The calculations also show that a low series resistance is less critical for high PCEs. This allows the application of alternative electrode materials and solar cell designs and may reduce the overall costs of the devices.

3. Determination of PCE

The characterization of solar cells operated under ambient artificial lighting such as FLs or LEDs has been very challenging.^[24,25] B. H. Hamadani et al.^[26,27] and S. Winter^[28] proposed an characterization procedure using a calibrated reference diode. Only recently, the International Electrotechnical Commission (IEC) has issued a technical specification for a device evaluation method for indoor light (IEC TS 62 607-7-2).^[29] The National Institute of Standard and Technology (NIST) does offer calibrated reference PV cells for indoor light measurements. NIST calibrates reference IPV cells for several different reporting conditions, including three different types of LED lighting and one fluorescent lighting source.^[30] However, as reference diodes and standardized light sources are not available in all laboratories, many researchers have used illuminance meters for the estimation of the irradiance and to report values in lux ($\text{lx} = \text{lm m}^{-2}$). Knowing the relative spectral intensity (RSI) distribution of the light source, Equation (2) can be used to calculate the light intensity. However, as two different light sources with identical illuminance at the measurement plane can have substantially different irradiance output, the electrical output of a solar cell characterized under the two light sources may be very different.

For a precise measurement of the PCE of a solar cell, the irradiance at the position of the device needs to be known. For the calculation of the illuminance, the spectral irradiance needs to be determined. In the following, a procedure is proposed that should allow a reliable characterization of solar cells under indoor conditions using a spectrum color meter, a lux meter, and a setup to measure the external quantum efficiency of the studied solar cell. In addition, a light source with a spectral irradiance matching the sensitivity of the color meter should be selected. As a first step, the illuminance of the light source at the sample position is measured using a calibrated lux meter. Ideally, a device with NIST traceable calibration is available for this measurement. The lux meter can also be used to check the lateral homogeneity of the illuminance. In the second step, the RSI is measured using a full-spectrum color meter. For this, measurement devices used in photography can be used. The measured illuminance and RSI allow the calculation of the intensity, the spectral irradiance, and the spectral photon flux (Φ_{LS}) at the sample location. External quantum efficiency (EQE_{PV}) is a standard measurement in laboratories manufacturing PV devices. Usually, the spectral photocurrent of a reference diode and the device of interest are measured, which allows the calculation of EQE_{PV} . Using Equation (1a), the photocurrent density of the solar cell, expected for the photon flux Φ_{LS} can be calculated. In the last step, the solar cell is placed in the same position the illuminance and RSI were measured and a current density–voltage curve is recorded. The characterization procedure is summarized in **Figure 3**.^[31]

The measured short-circuit current density and the calculated photocurrent density should be identical. Large deviations between the calculated and the measured current densities indicated inconsistencies in the measurement procedure and suggested a poor accuracy of the derived device efficiency. Repeating the measurements at different light intensities can be used to improve the confidence level of the experimental data. Similar to the characterization of solar cells under AM1.5G, deviations of $\pm 5\%$ between the measured and the calculated short-circuit current can be considered to be sufficient.

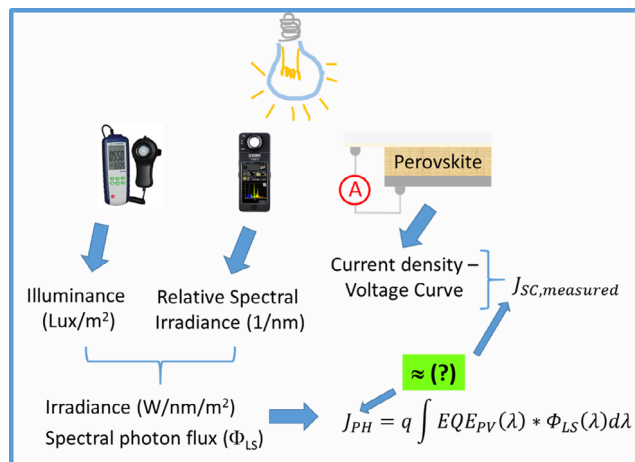


Figure 3. Indoor efficiency measurement procedure.

4. Indoor Efficiencies of Emerging PV Technologies

To estimate the efficiency limit of state-of-the-art solar cells, in addition to the losses discussed earlier, optical losses need to be considered. This can be done by reducing the EQE_{PV} . Best solar cells show external quantum efficiencies in the range of 85%–90%.^[32] Including the reduced EQE_{PV} into the calculations earlier, one expects PCEs in the range of $\approx 40\%$ for perovskite solar cells ($EQE_{EL} \approx 0.1\%$) and $\approx 30\%$ for organic and dye-sensitized solar cells when the bandgap of the absorber and the emission spectrum are well matched and a light source with broad emission in the visible spectral range delivering 1000 lux illuminance at the sample position are assumed. Even higher efficiencies can be achieved when light sources with more intensity in the red and near-infrared spectral region are applied. For a narrow emission between 600 and 700 nm with an illuminance of 1000 Lux (Figure S1, Supporting Information), a PCE $> 60\%$ is calculated (Figure S4, Supporting Information). The spectral shift leads to higher photocurrents with similar open-circuit voltages and electrical fill factors. The higher light intensity also supports the efficiency increase.

Indoor efficiencies reported in the literature (Table 1) are in good agreement with the performed calculations. Although different light sources, light intensities, and measurement conditions were applied making a direct comparison difficult, a PCE of $\approx 40\%$ was reported for perovskite solar cells, and 30%–40% PCE was found for organic and dye-sensitized devices.

In addition to a bandgap optimization, the most promising approach to increase the indoor PCE of perovskite, organic, and dye-sensitized solar cells is the reduction of non-radiative recombination. This can be achieved by developing more emissive semiconductors, by the reduction and/or passivation of bulk and surface defects, and by the optimization of the semiconductor–contact interfaces. Increasing EQE_{EL} is also one of the key research strategies of the solar PV community. Although the bandgap of semiconductors used in optimized outdoor and indoor solar cells will be different, novel interface materials or defect passivation moieties developed for outdoor solar cells may also be useful for indoor devices. For organic solar cells, the introduction of non-fullerene acceptors has led to more radiative recombination compared to the solar cells with a donor polymer and a fullerene acceptor.^[19] Although non-radiative recombination is still the dominant process even in OPVs with a PCE of 18%, designing new electron acceptor materials is a promising strategy to enhance radiative recombination in OPVs. The bandgaps of various emerging PV technologies

can easily be tuned. For organic solar cells, the π -conjugated structure of the donor and the acceptor, and for dye-sensitized solar cells, the chemical structure of the dye adsorbed to the nanoporous TiO_2 determine the bandgap of the absorber layer. Several different approaches are available to tune the optical properties of perovskites.^[33] A partial substitution of iodide by bromide ions, using different cations, or building 2D/3D perovskite crystals are among the most popular approaches.

Overall, perovskite PV devices appear to be the most promising candidates for indoor applications at the moment. In the last few years, a lot of progress has been made in reducing the efficiency losses in these devices. However, most perovskite devices are based on lead-containing salt leading to environmental and health concerns. It is still unclear whether or not they can be integrated into disposable consumer products and deployed on a large scale. Organic and dye-sensitized solar cells are also excellent candidates for IPV applications. Both have been manufactured on a small scale for several years. Their environmental impact is expected to be much smaller compared to perovskite solar cells. All three technologies have in common that the manufacturing costs are still not fully understood. Especially for indoor products, only small volumes will be manufactured and it will be difficult to utilize any economy of scale.

5. Summary

In this manuscript, the PCE of PV devices operated under typical indoor conditions was discussed. By applying a simple model including the effect of non-radiative recombination and Ohmic losses, the maximum conversion efficiencies were calculated. An alignment of the absorption spectrum of the device and the emission spectrum of the used light source and very low levels of non-radiative recombination are essential to achieve high PCEs. The model is also used to estimate the indoor performance of perovskite, organic, and dye-sensitized solar cells. Efficiencies in the range of 35%–45% are found which is in good agreement with data reported in the literature. The calculations also show that the calculation results are very sensitive to the applied light source.

Overall, perovskite, organic, and dye-sensitized solar cells appear to be good candidates for indoor applications. Their environmental impact and the manufacturing costs may decide which technology will be commercialized first.

Supporting Information

Supporting Information is available from the Wiley Online Library or from the author.

Acknowledgements

M.S. would like to thank the Austrian Research Promotion Agency (FFG) for financial support (Project ID 896686).

Conflict of Interest

The author declares no conflict of interest.

Table 1. Indoor efficiencies of different PV technologies.

PV technology	Indoor efficiency [%]	Illumination ^{a)}	Reference
Amorphous silicon PV	19–21	1000 Lux LED	[34]
Dye-sensitized PV	38	1000 Lux FL	[31]
Organic PV	31	1650 Lux LED	[35]
Perovskite PV	41.2	1062 Lux LED	[36]
Quantum dot PV	19.5	2000 Lux FL	[37]

^{a)}FL = fluorescent lamp and LED = light emitting diode.

Data Availability Statement

The data that support the findings of this study are available from the corresponding author upon reasonable request.

Keywords

emerging photovoltaic technologies, indoor, power conversion efficiencies, solar cells

Received: October 8, 2023
Revised: November 15, 2023
Published online:

- [1] A. Sadeghi-Niaraki, *Future Gener. Comput. Syst.* **2023**, *143*, 361.
- [2] A. Chatterjee, C. N. Lobato, H. Zhang, A. Bergne, V. Esposito, S. Yun, A. R. Insinga, D. V. Christensen, C. Imbaquingo, R. Bjørk, H. Ahmed, M. Ahmad, C. Y. Ho, M. Madsen, J. Chen, P. Norby, F. M. Chiabrera, F. Gunkel, Z. Ouyang, N. Pryds, *J. Phys. Energy* **2023**, *5*, 022001.
- [3] N. Jaziri, A. Boughamoura, J. Müller, B. Mezghani, F. Tounsi, M. Ismail, *Energy Rep.* **2020**, *6*, 264.
- [4] Y. Wang, L. Yang, X. L. Shi, X. Shi, L. Chen, M. S. Dargusch, J. Zou, Z. G. Chen, *Adv. Mater.* **2019**, *31*, 1807916.
- [5] A. Nozariasbmarz, H. Collins, K. Dsouza, M. H. Polash, M. Hosseini, M. Hyland, J. Liu, A. Malhotra, F. M. Ortiz, F. Mohaddes, V. P. Ramesh, Y. Sargolzaeiaval, N. Snouwaert, M. C. Özturk, D. Vashae, *Appl. Energy* **2020**, *258*, 114069.
- [6] E. L. Pradeesh, S. Udhayakumar, M. G. Vasundhara, V. Vadivel Vivek, *IOP Conf. Ser.: Mater. Sci. Eng.* **2020**, *995*, 012007.
- [7] P. Munirathinam, A. Anna Mathew, V. Shanmugasundaram, V. Vivekananthan, Y. Purusothaman, S.-J. Kim, A. Chandrasekhar, *Mater. Sci. Eng., B* **2023**, *297*, 116762.
- [8] H. H. Ibrahim, M. J. Singh, S. S. Al-Bawri, S. K. Ibrahim, M. T. Islam, A. Alzamil, M. S. Islam, *Sensors* **2022**, *22*, 4144.
- [9] B. Li, B. Hou, G. A. J. Amaratunga, *InfoMat* **2021**, *3*, 445.
- [10] <https://www.nrel.gov/grid/solar-resource/spectra-am1.5.html> (accessed: October 2023).
- [11] <https://www.nrel.gov/pv/cell-efficiency.html> (accessed: October 2023).
- [12] O. Almora, D. Baran, G. C. Bazan, C. I. Cabrera, S. Erten-Ela, K. Forberich, F. Guo, J. Hauch, A. W. Y. Ho-Baillie, T. J. Jacobsson, R. A. J. Janssen, T. Kirchartz, N. Kopidakis, M. A. Loi, R. R. Lunt, X. Mathew, M. D. McGehee, J. Min, D. B. Mitzi, M. K. Nazeeruddin, J. Nelson, A. F. Nogueira, U. W. Paetzold, B. P. Rand, U. Rau, H. J. Snaith, E. Unger, L. Vaillant-Roca, C. Yang, H. Yip, et al., *Adv. Energy Mater.* **2023**, *13*, 2203313.
- [13] J. Min, S. Demchyshyn, J. R. Sempionatto, Y. Song, B. Hailegnaw, C. Xu, Y. Yang, S. Solomon, C. Putz, L. E. Lehner, J. F. Schwarz, C. Schwarzinger, M. C. Scharber, E. Shirzaei Sani, M. Kaltenbrunner, W. Gao, *Nat. Electron.* **2023**, *6*, 630.
- [14] W. Shockley, H. J. Queisser, *J. Appl. Phys.* **1961**, *32*, 510.
- [15] U. Rau, *Phys. Rev. B* **2007**, *76*, 085303.
- [16] K. Vandewal, K. Tvingstedt, A. Gadisa, O. Inganäs, J. V. Manca, *Nat. Mater.* **2009**, *8*, 904.
- [17] W. Tress, N. Marinova, O. Inganäs, M. K. Nazeeruddin, S. M. Zakeeruddin, M. Graetzel, *Adv. Energy Mater.* **2015**, *5*, 1400812.
- [18] B. Hailegnaw, S. Paek, K. T. Cho, Y. Lee, F. Ongül, M. K. Nazeeruddin, M. C. Scharber, *Sol. RRL* **2019**, *3*, 1900126.
- [19] J. Hofinger, C. Putz, F. Mayr, K. Gugujonovic, D. Wielend, M. C. Scharber, *Mater. Adv.* **2021**, *2*, 4291.
- [20] Y. Udum, P. Denk, G. Adam, D. H. Apaydin, A. Nevosad, C. Teichert, M. S. White, N. S. Sariciftci, M. C. Scharber, *Org. Electron.* **2014**, *15*, 997.
- [21] U. Hoyer, M. Wagner, T. Swonke, J. Bachmann, R. Auer, A. Osvet, C. J. Brabec, *Appl. Phys. Lett.* **2010**, *97*, 233303.
- [22] J. Bachmann, C. Buerhop-Lutz, C. Deibel, I. Riedel, H. Hoppe, C. J. Brabec, V. Dyakonov, *Sol. Energy Mater. Sol. Cells* **2010**, *94*, 642.
- [23] Y. Galagan, T. M. Eggenhuisen, M. J. J. Coenen, A. F. K. V. Biezemans, W. J. H. Verhees, S. C. Veenstra, W. A. Groen, R. Andriessen, R. A. J. Janssen, *J. Mater. Chem. A* **2015**, *3*, 20567.
- [24] B. Hamadani, in *2020 47th IEEE Photovoltaic Specialists Conf. (PVSC)*, IEEE, Piscataway, NJ **2020**, pp. 0333–0336, <https://doi.org/10.1109/PVSC45281.2020.9300935>.
- [25] P. R. Michael, D. E. Johnston, W. A. Moreno, *IEEE Instrum. Meas. Mag.* **2023**, *26*, 52.
- [26] B. H. Hamadani, M. B. Campanelli, *IEEE J. Photovoltaics* **2020**, *10*, 1119.
- [27] V. Pecunia, S. R. P. Silva, J. D. Phillips, E. Artagiani, A. Romeo, H. Shim, J. Park, J. H. Kim, J. S. Yun, G. C. Welch, B. W. Larson, M. Creran, A. Laventure, K. Sasitharan, N. Flores-Diaz, M. Freitag, J. Xu, T. M. Brown, B. Li, Y. Wang, Z. Li, B. Hou, B. H. Hamadani, E. Defay, V. Kovacova, S. Glinsek, S. Kar-Narayan, Y. Bai, D. B. Kim, Y. S. Cho, et al., *J. Phys. Mater.* **2023**, *6*, 042501.
- [28] S. Winter, *Indoor Photovoltaics*, John Wiley & Sons, Inc., Hoboken, NJ **2020**, pp. 115–131, <https://doi.org/10.1002/9781119605768.ch5>.
- [29] <https://webstore.iec.ch/publication/61819> (accessed: October 2023).
- [30] <https://www.nist.gov/sri/standard-reference-instruments/sri-6014-calibrated-reference-photovoltaic-cell> (accessed: October 2023).
- [31] H. Michaels, M. Rinderle, I. Benesperi, R. Freitag, A. Gagliardi, M. Freitag, *Chem. Sci.* **2023**, *14*, 5350.
- [32] M. A. Green, E. D. Dunlop, G. Siefert, M. Yoshita, N. Kopidakis, K. Bothe, X. Hao, *Prog. Photovoltaics Res. Appl.* **2023**, *31*, 3.
- [33] Z. Hu, Z. Lin, J. Su, J. Zhang, J. Chang, Y. Hao, *Sol. RRL* **2019**, *3*, 1900304.
- [34] M. Li, F. Igbari, Z. Wang, L. Liao, *Adv. Energy Mater.* **2020**, *10*, 2000642.
- [35] L.-K. Ma, Y. Chen, P. C. Y. Chow, G. Zhang, J. Huang, C. Ma, J. Zhang, H. Yin, A. M. Hong Cheung, K. S. Wong, S. K. So, *Joule* **2020**, *4*, 1486.
- [36] K. Wang, H. Lu, M. Li, C. Chen, D. Bo Zhang, J. Chen, J. Wu, Y. Zhou, X. Wang, Z. Su, Y. Shi, Q. Tian, Y. Ni, X. Gao, S. M. Zakeeruddin, M. Grätzel, Z. Wang, L. Liao, *Adv. Mater.* **2023**, *35*, 2210106.
- [37] B. Hou, B.-S. Kim, H. K. H. Lee, Y. Cho, P. Giraud, M. Liu, J. Zhang, M. L. Davies, J. R. Durrant, W. C. Tsoi, Z. Li, *Adv. Funct. Mater.* **2020**, *30*, 2004563.